



ELSEVIER

Available online at www.sciencedirect.com

SCIENCE @ DIRECT®

Journal of Organometallic Chemistry 666 (2003) 49–53

Journal
of Organo
metallic
Chemistrywww.elsevier.com/locate/jorgchem

Intermolecular hydrogen-bonding in the solid-state structure of $\text{CpFe}(\text{CN})_2(\text{PTAH})$ Structural and spectral comparisons with its $[\text{K}][\text{CpFe}(\text{CN})_2\text{PTA}]$ salt

Donald J. Darensbourg*, Andrea L. Phelps, M. Jason Adams, Jason C. Yarbrough

Department of Chemistry, Texas A&M University, College Station, TX 77843, USA

Received 29 July 2002

Dedicated to Professor Jerry L. Atwood on the occasion of his 60th birthday

Abstract

The salt $[\text{K}][\text{CpFe}(\text{CN})_2\text{PTA}]$ (**1**) has been synthesized from the photolysis of $[\text{K}][\text{CpFe}(\text{CN})_2\text{CO}]$ and 1,3,5-triaza-7-phosphaadamantane (PTA) in methanol. Protonation of the salt by hydrogen ion exchange employing DOWEX 50 WX8-100 ion exchange resin yielded the complex $\text{CpFe}(\text{CN})_2\text{PTAH}$ (**2**). The solid-state structures of both compounds have been determined by X-ray crystallography. Protonation was shown via $\nu(\text{CN})$ and ^{31}P -NMR to occur at one of the PTA nitrogens. Furthermore, it was found in the solid-state of the protonated structure that intermolecular hydrogen-bonding occurs between the cyanide nitrogen of one molecule and the PTA nitrogen of another molecule. The average $\text{Fe}-\text{C}_{\text{CN}}$ distance for **1** is 1.877(11) Å. $\text{Fe}-\text{C}_{\text{CN}}$ distances for complex **2** differ significantly at 1.839(12) and 1.940(12) Å, with the shorter bond length associated with the hydrogen-bonded CN group. Spectral ($\nu(\text{CN})$ and ^{31}P -NMR) characterization of the complexes and their potential use as precursors to double metal cyanide derivatives are reported.

© 2002 Elsevier Science B.V. All rights reserved.

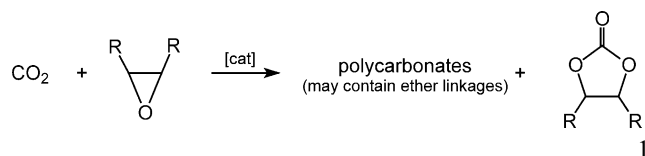
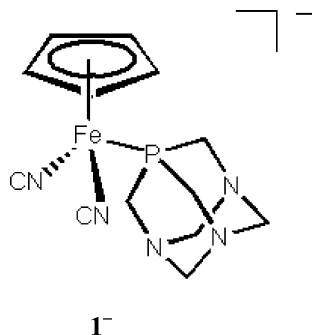
Keywords: Anionic organometallic cyanides; Protonated phosphine iron cyanides; Intermolecular hydrogen-bonding

1. Introduction

A focus of our research efforts is the metal-catalyzed coupling of carbon dioxide and epoxides to provide polycarbonates and/or cyclic carbonates (Eq. (1)) [1]. Pertinent to this subject the patent literature contains a plethora of references to the use of heterogeneous double metal cyanides (DMC) catalysts for the homopolymerization of epoxide to polyethers or the copolymerization of epoxides and carbon dioxide to polycarbonates [2]. These catalyst systems are comprised of a metal ion (M^1) which is capable of forming strong bonds to oxygen and a metal (M^2) cyanide salt, e.g. $[\text{M}^1]_n[\text{M}^2(\text{CN})_6]_m$. Prominent among these catalysts is $[\text{Zn}]_3[\text{Fe}(\text{CN})_6]_2$. Nevertheless, there have been few

attempts aimed at rationalizing the structural/reactivity function of these catalysts. In this regard we have communicated our initial thoughts on this matter employing the molecular complex $[\text{CpFe}(\mu\text{-CN})_2\text{ZnI}(\text{THF})]_2-\mu\text{-dppp}$, where dppp = diphenylphosphinopropane [3]. Herein, we wish to report the syntheses and structural characterization of precursor complexes to DMC derivatives, namely $[\text{K}][\text{CpFe}(\text{CN})_2\text{PTA}]$ (**1**) and $[\text{H}][\text{CpFe}(\text{CN})_2\text{PTA}]$ (**2**) (PTA = 1,3,5-triaza-7-phosphaadamantane) (**3**). In general the protonated form of these anionic organometallic cyanides are particularly useful in the synthesis of DMC derivatives in that they eliminate accompanying salt formation and difficulties associated with its removal. Interestingly, on a totally unrelated note, in the solid-state, complex **2** has an important structural feature, *intermolecular hydrogen-bonding*, like that seen in the $[\text{Fe}(\text{CN})_2\text{CO}]$ unit present in $[\text{NiFe}]$ hydrogenase [4,5b].

* Corresponding author



2. Experimental

All manipulations were performed under Ar using standard Schlenk and glovebox techniques. Solvents were distilled from the appropriate reagents before use. DOWEX 50 WX8-100 ion exchange resin (Aldrich) was washed with MeOH and dried in vacuo. $K[CpFe(CO)(CN)_2]$ [5] and 1,3,5-triaza-7-phosphaadamantane (PTA) [6] were prepared according to published procedures.

IR spectra were recorded on a Mattson 6021 FTIR using a 0.1 mm CaF_2 -sealed cell for solution and KBr pellets for solid samples. ^{31}P -NMR spectra were measured on a Varian Unity Plus 300 MHz spectrometer (121.4 MHz ^{31}P). The magnetic field was locked with D_2O and an 85% H_3PO_4 solution was used as an external reference.

2.1. Synthesis of $K[CpFe(CN)_2PTA]$ (**1**)

$K[CpFe(CN)_2CO]$ (0.480 g, 2.0 mmol) and PTA (0.347 g, 2.0 mmol) were dissolved in MeOH (100 ml) in a photolysis vessel. An Ar purge was bubbled through the solution as it was irradiated for 30 min with UV light from a Hg arc 450W UV Hanovia immersion lamp. A color change from yellow to orange occurred. The solvent was removed in vacuo. The orange solid was washed several times with acetone. X-ray quality crystals were obtained by slow evaporation of a MeOH solution at room temperature (r.t.). Yield: 0.365 g, 49%. ^{31}P -NMR (MeOH): $\delta = 9.4$ ppm. IR (KBr): ν CN 2048, 2033 cm^{-1} . (H_2O): ν CN 2039, 2018 cm^{-1} . (MeOH): ν CN 2051, 2036 cm^{-1} .

2.2. Synthesis of $CpFe(CN)_2PTAH$ (**2**)

$K[CpFe(CN)_2PTA]$ (0.050 g, 0.14 mmol) was dissolved in 10 ml MeOH. The solution was transferred to 2 g DOWEX 50 WX8-100 ion exchange resin. The solution was stirred for 30 s. A color change from orange to pale yellow occurred. The solution was separated from the DOWEX and solvent removed in vacuo. X-ray quality crystals were obtained by slow evaporation of a MeOH solution at r.t. ^{31}P -NMR (MeOH): $\delta = 20$ ppm. IR (KBr): ν CN 2056, 2042 cm^{-1} . (H_2O): ν CN 2046, 2029 cm^{-1} . (MeOH): ν CN 2058, 2043 cm^{-1} .

2.3. Reaction of complex **2** with $Zn(N(SiMe_3)_2)_2$

$CpFe(CN)_2PTAH$ (0.086 g, 0.26 mmol) was dissolved in 15 ml THF. $Zn(N(SiMe_3)_2)_2$ (0.100 g, 0.26 mmol) in 10 ml THF was transferred to the flask containing the $CpFe(CN)_2PTAH$, immediately followed by the addition of 2,4,6-tri-*t*-butylphenol (0.068 g, 0.26 mmol) also in THF. As the solution stirred, it became cloudy with the formation of a yellow precipitate. The precipitate was not soluble in any common solvent, and is formulated as a Zn–Fe cyanide bridged aggregate much like that observed in Ref. [3]. KBr (ν CN): 2091, 2062 cm^{-1} .

2.4. X-ray crystallography

Each sample was coated with a cryogenic protectant (i.e. paratone) and mounted on a glass fiber, which in turn was fashioned to a Cu mounting pin. The crystal was then placed in a cold nitrogen stream (Oxford) maintained at 110 K. The X-ray data were obtained on a Bruker CCD diffractometer and covered more than a hemisphere of reciprocal space by a combination of three sets of exposures; each exposure set had a different angle ϕ for the crystal orientation and each exposure covered 0.3° in ω . The crystal-to-detector distance was 4.9 cm. Crystal decay was monitored by repeating the data collection for initial frames at the end of the data set and analyzing the duplicate reflections; crystal decay was negligible. The space group was determined based on systematic absences and intensity statistics [7].

Crystal data and details of data collection are provided in Table 1. Selected bond distances and angles are given in Table 2. The structures were solved by direct methods. Full-matrix least-squares anisotropic refinement for all non-hydrogen atoms yielded $R(F)$ and $wR(F^2)$ values as indicated in Table 1 at convergence. All H atoms were placed at idealized positions and refined with fixed isotropic displacement parameters equal to 1.2 (1.5 for methyl protons) times the equivalent isotropic displacement parameters of the atoms to which they were attached. Neutral atom scattering

Table 1
X-ray crystallographic data for $K[CpFe(CN)_2PTA]$ and $CpFe(CN)_2PTAH$

	$K[CpFe(CN)_2PTA]$ (1)	$CpFe(CN)_2PTAH$ (2)
Empirical formula	$C_{13}H_{17}FeKN_5P \cdot KCN$	$C_{13}H_{18}FeN_5P$
Formula weight (g mol ⁻¹)	434.35	331.13
Temperature (K)	110	110
Wavelength (Å)	0.71073	0.71073
Space group	$P2_1/c$	$P2_1/c$
<i>a</i> (Å)	13.867(6)	7.263(6)
<i>b</i> (Å)	7.413(3)	12.809(10)
<i>c</i> (Å)	17.561(7)	15.247(12)
α (°)	–	–
β (°)	90.969(9)	103.263(15)
γ (°)	–	–
Volume (Å ³)	1805.0(13)	1380.6(18)
<i>Z</i>	4	4
<i>D</i> _{calc} (g cm ⁻³)	1.598	1.588
Absolute coefficient (mm ⁻¹)	1.394	1.205
<i>R</i> ^a	8.10	7.09
<i>R</i> _w ^b	18.87	15.59
Goodness-of-fit on <i>F</i> ²	0.816	0.871

$$^a R = \sum ||F_o| - |F_c|| / \sum |F_o|$$

$$^b R = \{[\sum w(F_o^2 - F_c^2)^2] / [\sum w(F_o^2)^2]\}^{1/2}$$

Table 2
Selected bond lengths (Å) and angles (°) for $K[CpFe(CN)_2PTA]$ and $CpFe(CN)_2PTAH$

	$K[CpFe(CN)_2PTA]$	$CpFe(CN)_2PTAH$
<i>Bond lengths</i>		
Fe–C(6)	1.864(9)	1.839(12)
Fe–C(7)	1.871(10)	1.940(12)
N(1)–C(6)	1.174(10)	1.189(12)
N(2)–C(7)	1.167(11)	1.115(11)
Fe–Cp (av)	2.092(10)	2.096(11)
Fe–P	2.145(3)	2.128(3)
N(1)–K	2.768(7)	–
N(2)–K	2.802(7)	–
N(4)–N(1A)	–	2.686
<i>Bond angles</i>		
Fe–C(6)–N(1)	177.7(8)	178.2(10)
Fe–C(7)–N(2)	177.7(7)	176.0(10)

factors and anomalous scattering factors were taken from the International Tables for X-ray Crystallography Vol. C.

For complexes **1** and **2**, data reduction: SAINTPLUS (Bruker [8]); program used to solve the structure: SHELXS-86 (Sheldrick [9]); programs used to refine the structure: SHELXL-97 (Sheldrick [10]); program used for molecular graphics: SHELXTL version 5.0 (Bruker [7]); software used to prepare material for publication: SHELXTL version 5.0 (Bruker [11]).

3. Results and discussion

The phosphine derivative, $[K][CpFe(CN)_2PTA]$ (**1**), was prepared by photolysis of $[K][CpFe(CN)_2CO]$ and PTA in methanol solution where the reactants are soluble. The reaction was readily monitored by observing the disappearance of the $\nu(CN)$ and $\nu(CO)$ bands in the starting complex (2093, 2082, and 1972 cm⁻¹) and the concomitant appearance of the two $\nu(CN)$ bands in the product (2051 and 2036 cm⁻¹) by infrared spectroscopy. An orange solid product was isolated upon removal of the methanol, which was washed with acetone and dried under vacuum to provide **1** in a 49% yield. The ³¹P-NMR chemical shift of the anion of complex **1** in methanol was observed at 9.4 ppm, which is shifted significantly downfield from that of free PTA in methanol at –97 ppm.

X-ray quality crystals of **1** were obtained by the slow evaporation of a methanol solution of the complex at ambient temperature. A thermal ellipsoid drawing of the anion of **1** is depicted in Fig. 1, along with the atomic numbering scheme. Selected bond distances and angles are listed in Table 2. The $[CpFe(CN)_2PTA]$ anion is a typical three-legged piano stool with linear Fe–CN groups. The average Fe–C_{Cp} distance is 2.092(10) Å, the two Fe–C_{CN} distances are quite similar at 1.864(9) and 1.871(10) Å, and the Fe–P distance is 2.145(3) Å. The C–N distances are typical, averaging 1.171(12) Å. As was observed in the $[K][CpFe(CN)_2CO]$ salt, the structure of **1** shows extensive contact ion pairing interactions between K⁺ and cyanide (av. K⁺⋯NC distance = 2.785(7) Å).

Direct protonation of complex **1** with HCl leads to coproduction of KCl. Since both the desired product, $CpFe(CN)_2PTAH$ (**2**), and KCl are highly water soluble it was difficult to purify the product. Hence, we resorted to replace potassium in **1** with hydrogen utilizing a Dowex-50W-hydrogen, strongly acidic cation exchange resin. This technique resulted in the production of a pale yellow complex **2** in near quantitative yield. The $\nu(CN)$

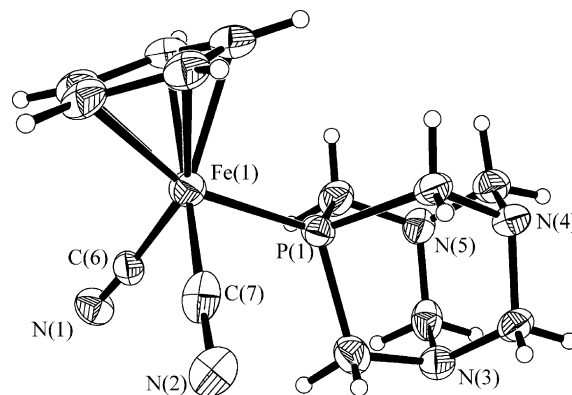


Fig. 1. Thermal ellipsoid representation of the anion of complex **1**, $CpFe(CN)_2PTA^-$.

vibrations of **2** in methanol appear at slightly higher frequencies (2058 and 2043 cm^{-1}) relative to the corresponding values in the potassium salt. On the other hand, the ^{31}P -NMR chemical shift in **2** in methanol is observed at 20 ppm, some 11 ppm downfield from that in **1**. These observations are strong evidence that protonation occurs at one of the nitrogen centers of the PTA ligand [12] as opposed to the nitrogen center on one of the cyanide ligands as in $[\text{H}][\text{CpFe}(\text{CO})(\text{CN})_2]$ [5b].

Crystals of complex **2** were obtained by the slow evaporation of a methanol solution of the derivative at ambient temperature. A thermal ellipsoid representation of **2** is depicted in Fig. 2, along with the atomic numbering scheme. Selected bond distances and angles are provided in Table 2. The average $\text{Fe}-\text{C}_{\text{cp}}$ and $\text{Fe}-\text{P}$ distances in complex **2** at 2.096(11) and 2.128(3) Å, respectively are quite similar to the corresponding values in complex **1**. On the other hand, whereas the two $\text{Fe}-\text{C}_{\text{CN}}$ distances are essentially identical in **1** having an average value of 1.877 Å [11] they differ significantly in **2**, i.e. $\text{Fe}-\text{C}(6)$ at 1.839(12) Å is ca. 0.1 Å shorter than $\text{Fe}-\text{C}(7)$ at 1.940(12) Å. Interestingly, the shorter $\text{Fe}-\text{C}_{\text{CN}}$ bond is associated with an *intermolecular* hydrogen-bonding chain motif which traverses the crystal involving the protonated nitrogen atom of the PTA ligand, with a $-\text{CN}(1\text{A})\cdots\text{N}(4)$ distance of 2.686 Å. This represents a rather strong hydrogen bond, considerably shorter than the sum of the van der Waals radii of two nitrogen atoms. This intersection is revealed as well in the solid-state (KBr) infrared spectra in the

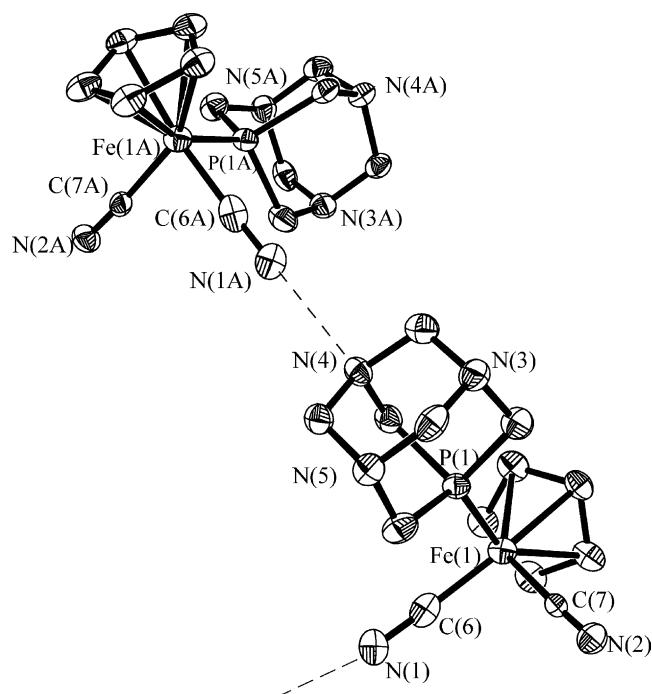


Fig. 2. Thermal ellipsoid representation of complex **2**, $\text{CpFe}(\text{CN})_2\text{PTAH}$.

$\nu(\text{CN})$ region, where the frequencies in complex **2** are 8–9 cm^{-1} higher than those of complex **1**. In $[\text{H}][\text{CpFe}(\text{CO})(\text{CN})_2]$, where both cyanide ligands in the solid-state are involved in intermolecular hydrogen-bonding, the average $\text{Fe}-\text{C}_{\text{CN}}$ distances are 1.861 [6] versus 1.911 Å [8] in the potassium salt. Nevertheless, a more substantial shift of the $\nu(\text{CN})$ vibrational modes in KBr to higher frequencies is observed upon hydrogen-bonding, from 2085 and 2095 cm^{-1} to 2106 and 2135 cm^{-1} [5b]. In this instance the $-\text{CN}\cdots\text{NC}-$ separation is 2.55 Å, typical of strong hydrogen-bonding [13,14]. Hence, in both derivatives strong hydrogen-bonding to the cyanide ligands leads to an increase in $\nu(\text{CN})$ and a decrease in $\text{Fe}-\text{C}_{\text{CN}}$ bond length.

Relevant to the site of protonation in the $\text{CpFe}(\text{CN})_2\text{PTA}^-$ anion, free PTA has a $\text{p}K_{\text{a}}$ in water of 5.70, with the nitrogen centers in metal-bound PTA expected to be less basic [12]. Hence, the cyanide ligands in $\text{CpFe}(\text{CN})_2\text{PTA}^-$ by necessity must have a $\text{p}K_{\text{a}}$ value in water less than 5.70 which is significantly smaller than that of HCN where the $\text{p}K_{\text{a}}$ is 9.31. This observation is consistent with CNH being a stronger acid than HCN by 10–20 kcal mol^{-1} [13]. Indeed, the $\text{p}K_{\text{a}}$ of the cation $\text{trans-Fe}(\text{H}_2)(\text{CNH})(\text{depe})_2^{+2}$ has been determined to be ca. 2.7 in water [15]. The $\nu(\text{CN})$ vibrational frequencies of complexes **1** and **2** in water, where hydrogen-bonding occurs at basic sites, are significantly lower than the values in methanol, but do not differ dramatically from one another at 2039 and 2018 cm^{-1} , and 2046 and 2029 cm^{-1} , respectively. The slightly higher values for the $\nu(\text{CN})$ modes in complex **2** result from the fact that the PTA ligand is protonated.

Initial attempts at employing complex **2** in the synthesis of mixed metal cyanide derivatives has involved its reaction with $\text{Zn}(\text{N}(\text{SiMe}_3)_2)_2$. This reaction has provided a species which appears to exist as an aggregate. That is, it is insoluble in common organic solvents. The $\nu(\text{CN})$ solid-state infrared spectrum of the species displays bands at 2091 and 2062 cm^{-1} which are shifted 43 and 29 cm^{-1} , respectively to higher frequencies as compared with the corresponding values in complex **1**, consistent with bridging cyanide groups. Efforts to fully characterize this derivative are underway.

4. Supplementary material

Crystallographic data for the structural analyses have been deposited with the Cambridge Crystallographic Data Centre, CCDC nos. 192638–192639 for complexes **1** and **2**. Copies of the information may be obtained free of charge from The Director, CCDC, 12 Union Road, Cambridge CB2 1EZ, UK (Fax: +44-1223-336033; e-

mail: deposit@ccdc.cam.ac.uk or [www: http://www.ccdc.cam.ac.uk](http://www.ccdc.cam.ac.uk)).

Acknowledgements

Financial support from the National Science Foundation (CHE-99-10342 and CHE 98-07975 for the purchase of X-ray equipment), the R.A.W. Foundation, and by the Texas Advanced Research Technology Program (Grant No. 0390-1999) is greatly appreciated.

References

- [1] (a) D.J. Darensbourg, M.W. Holtcamp, *Macromolecules* 28 (1995) 7577;
(b) D.J. Darensbourg, M.W. Holtcamp, G.E. Struck, M.S. Zimmer, S.A. Niezgoda, P. Rainey, J.B. Robertson, J.D. Draper, J.H. Reibenspies, *J. Am. Chem. Soc.* 121 (1999) 107;
(c) D.J. Darensbourg, J.R. Wildeson, J.C. Yarbrough, J.H. Reibenspies, *J. Am. Chem. Soc.* 122 (2000) 12487.
- [2] (a) W.J. Kruper, D.J. Swart, US Patent 4,500,704, 1985;
(b) B. Le-Khac, US Patent 5,482,908, 1996;
(c) P. Ooms, J. Hofmann, P. Gupta, US Patent 6,204,357, 2001;
(d) B. Le-Khac, US Patent 6,211,330, 2001;
(e) J. Hofmann, P. Ooms, P. Gupta, W. Schafer, US Patent 6,291,338, 2001.
- [3] D.J. Darensbourg, M.J. Adams, J.C. Yarbrough, *Inorg. Chem.* 40 (2001) 6543.
- [4] (a) M. Frey, *Struct. Bonding* 90 (1998) 97 (and references therein);
(b) J.C. Fontecilla-Camps, *J. Biol. Inorg. Chem.* 1 (1996) 91 (and references therein);
(c) A. Volbeda, E. Garcin, C. Piras, A.L. de Lacey, V.M. Fernandez, E.C. Hatchikian, M. Frey, J.C. Fontecilla-Camps, *J. Am. Chem. Soc.* 118 (1996) 12989;
(d) A. Volbeda, M.-H. Charon, C. Piras, E.C. Hatchikian, M. Frey, J.C. Fontecilla-Camps, *Nature* 373 (1995) 580;
(e) R.P. Happe, W. Roseboom, A.J. Pierik, S.P.J. Albracht, K.A. Bagley, *Nature* 385 (1997) 126;
(f) K.A. Bagley, E.C. Duin, W. Roseboom, S.P.J. Albracht, W.H. Woodruff, *Biochemistry* 34 (1995) 5527.
- [5] (a) C.E. Coffey, *J. Inorg. Nucl. Chem.* 25 (1963) 179;
(b) C.-H. Lai, W.-Z. Lee, M.L. Miller, J.H. Reibenspies, D.J. Darensbourg, M.Y. Darensbourg, *J. Am. Chem. Soc.* 120 (1998) 10103.
- [6] D.J. Daigle, A.B. Pepperman, S.R. Vail, Jr., *J. Heterocycl. Chem.* 17 (1974) 407.
- [7] SMART 1000 CCD, Bruker Analytical X-ray Systems, Madison, WI, 1999.
- [8] Bruker, SAINT-PLUS, Version 6.02, Madison, WI, USA, 1999.
- [9] G. Sheldrick, SHELXS-86 Program for Crystal Structure Solution, Institut für Anorganische Chemie der Universität Tammanstrasse 4, D-3400 Göttingen, Germany, 1986.
- [10] G. Sheldrick, SHELXL-97 Program for Crystal Structure Refinement, Institut für Anorganische Chemie der Universität, Tammanstrasse 4, D-3400 Göttingen, Germany, 1997.
- [11] Bruker, SHELXTL, Version 5.0, Madison, WI, USA, 1999.
- [12] D.J. Darensbourg, J.B. Robertson, D.L. Larkins, J.H. Reibenspies, *Inorg. Chem.* 38 (1999) 2473.
- [13] W.P. Fehlhammer, M. Fritz, *Chem. Rev.* 93 (1993) 1243.
- [14] S.M. Contakes, M. Schmidt, T.B. Rauchfuss, *Chem. Commun.* (1999) 1183.
- [15] T.P. Fong, C.E. Forde, A.J. Lough, R.H. Morris, P. Rigo, E. Rocchini, T. Stephan, *J. Chem. Soc. Dalton Trans.* (1999) 4475.